



## Electrocatalysis of Pt-Based Metal Loaded TiO<sub>2</sub> Modified Graphene Oxide for Methanol Oxidation

 S. Rattanakansang<sup>1,2</sup>, S. Themsirimongkon<sup>2,3</sup>, B. Kantalue<sup>4</sup>, B. Inceesungvorn<sup>2,3</sup>, S. Saipanya<sup>2,3</sup>, P. Waenkaew<sup>2,3\*</sup>
<sup>1</sup> Graduate School, Chiang Mai University, Chiang Mai 50200, Thailand

<sup>2</sup> Department of Chemistry and the Center of Innovation in Chemistry, Faculty of Science, Chiang Mai University, Chiang Mai 50200, Thailand

<sup>3</sup> Materials Science Research Center, Faculty of Science, Chiang Mai University, Chiang Mai 50200, Thailand

<sup>4</sup> Electron Microscope Research and Service center, Faculty of Science, Chiang Mai University, Chiang Mai, 50200, Thailand

\*Corresponding author's e-mail address: paralee.w@gmail.com (P. Waenkaew)

### ARTICLE INFO

#### Article history

Submitted: 10 February 2017

Revised: 3 July 2017

Accepted: 10 July 2017

Available online: 28 July 2017

#### Keywords:

Electrocatalyst

Electrodeposition

Graphene oxide

Methanol oxidation

Metal oxide

Titaniumdioxide

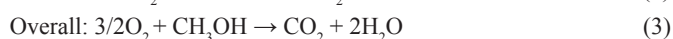
© 2017 The Microscopy Society of Thailand

### ABSTRACT

Titanium dioxide (TiO<sub>2</sub>) modified graphene oxide (GO) was prepared as a support for methanol oxidation reaction. Electrodeposition of platinum (Pt) and palladium (Pd) on the obtained TiO<sub>2</sub>-GO was then carried out to study their activities on methanol oxidation. Scanning electron microscopy (SEM) and transmission electron microscopy (TEM) with energy dispersive X-ray spectroscopy (EDS) were used to identify their morphologies and chemical compositions, respectively. It was found that, TiO<sub>2</sub> was successfully attached on GO surface and a narrow size distribution of Pt particles was found on TiO<sub>2</sub>-GO surface. EDS spectrum confirmed the presence of C, O, Ti, and Pt elements in the prepared catalysts. The electrocatalytic activities of the electrocatalysts toward oxidation of 0.5 M CH<sub>3</sub>OH in 0.5 M H<sub>2</sub>SO<sub>4</sub> solution were examined using cyclic voltammetry (CVs). For mono-metallic Pt catalysts, the addition of TiO<sub>2</sub> significantly enhanced methanol oxidation property and promoted CO tolerance performance. With exceptional activity and durability toward efficient methanol oxidation reaction, the forward current intensity, backward current intensity and onset potential of the 2Pt/TiO<sub>2</sub>-GO are 1.36 mA.cm<sup>-2</sup> and 0.98 mA.cm<sup>-2</sup> and 0.44 V vs.Ag/AgCl, respectively. Long-term stabilities of the electrocatalysts were examined by chronoamperometry (CAs). It was found that the 2Pt/TiO<sub>2</sub>-GO (0.019 mA.cm<sup>-2</sup>) showed higher current intensity than the 2Pt/GO catalyst (0.008 mA.cm<sup>-2</sup>). For bi-metallic xPt2Pd/TiO<sub>2</sub>-GO catalysts, their activities and stabilities are not outstanding but the 6Pt2Pd/TiO<sub>2</sub>-GO showed rather promising results in terms of lower potential and comparable current intensity to the 8Pt/TiO<sub>2</sub>-GO. Incorporation of Pd with Pt provided lower onset potential, lower potential at maximum current intensities (E<sub>c</sub>) and higher stabilities compared with the catalysts without Pd.

### INTRODUCTION

Nowadays, natural power resources are in high demand but a low supply is being confronted. There are a growing number of investigation groups devoted to discovering new resources. Fuel cells provide one option that is eco-friendly and cost-effective because the fundamental electrochemistry produces zero emissions and most of the consumed fuel sources are inexpensive [1]. Various types of fuel cells have been developed that use different electrolytes and fuel sources [2]. Direct methanol fuel cells (DMFC) are a technology that uses methanol as a source of energy. Methanol is liquid at room temperature, and is easy to handle and transport. Methanol also has good kinetics in oxidation compared to other alcohols. The DMFC is principally promising for portable electronics and vehicular applications. It consists of an anode where methanol is electro-oxidized to CO<sub>2</sub> and a cathode in which oxygen is reduced to water as shown in the following reaction equations [3].



Usually, Pt is used in fuel cells, but during the oxidation reaction it produces intermediates such as carbon monoxide (CO) species which is poisonous to Pt and can block the active catalytic sites. The reduction of this CO poisoning effect can be achieved by modifying the carbon support with some metal oxides such as cerium (IV) oxide (CeO<sub>2</sub>), titanium dioxide (TiO<sub>2</sub>), tungsten oxide (WO<sub>x</sub>), niobium oxide (NbO<sub>2</sub>), manganese dioxide (MnO<sub>2</sub>), cobalt (II,III) oxide (Co<sub>3</sub>O<sub>4</sub>) [4]. For this reason, the present work aims to use TiO<sub>2</sub> for preparation of the modified carbon support to improve the electro-catalytic activity. The strong interaction between Pt and TiO<sub>2</sub> on the carbon support has been found to result in the removal of poisoning species and the inhibition of Pt nanoparticles from migrating or detaching from the carbon support, which may be promising for catalyst development [4-6]. Additionally, great efforts have been focused on the development of bi-metallic catalysts by combining Pt and Pd which is relatively cost-effective to load on the metal oxide modified carbon. In the present work, a graphene oxide (GO) support modified with TiO<sub>2</sub> has been employed as a supporting material for Pt and Pd metal nanoparticles for enhancing electrocatalysis in methanol oxidation. The obtained catalysts were characterized by atomic force microscope (AFM), field emission scanning electron microscopy (FE-SEM), transmission electron microscope (TEM) with energy dispersive

X-ray spectrometer (EDS) and fourier transform infrared spectroscopy (FT-IR). Electrocatalytic performances of the prepared samples were investigated by cyclic voltammetry (CVs) and chronoamperometry (CA).

## METHODOLOGY

### Sample preparation

GO was synthesized by modified Hummers' method [7]. Briefly, 1 g of graphite was dispersed in 120 mL of conc.  $\text{HNO}_3$  and 180 mL of conc.  $\text{H}_2\text{SO}_4$ , and stirred in an ice bath for 1 h. Then, 0.5 g of  $\text{NaNO}_3$  was added and stirred for 20 min. After that, 3 g of  $\text{KMnO}_4$  was introduced into the suspension and stirred in a cold water bath for 1 h. Then, 530 mL of DI water was added into the suspension and stirred for 20 h. The oxidizing agent (5 mL of  $\text{H}_2\text{O}_2$ ) was subsequently dropped into the suspension, following by the addition of water to reach 1,000 mL by volume. The suspension was left overnight, and then washed with 1.0 M HCl and DI water several times to remove the remaining impurities [8-9]. The GO product was then obtained after drying at 65 °C. The GO was sonicated and stirred with DI water for 30 min respectively. The obtained GO was mixed with  $\text{TiO}_2$  in 10% wt, then sonicated and stirred overnight. Later on, the solution was centrifuged several times and dried at 65 °C. The composite of catalyst was dispersed in ink solution (2 mg of catalyst in the mixture of Nafion solution/ethanol/DI water in 6.25:20:73.75 volume ratio) to form a homogeneous suspension [10].

5  $\mu\text{L}$  of the ink was dropped onto the polished glassy carbon electrode (GCE). Electrodeposition of Pt and/or Pd on the obtained  $\text{TiO}_2$  modified GO was performed by scanning the potential in the range of -0.40 to 1.0 V at room temperature in 1 mM  $\text{H}_2\text{PtCl}_6 \cdot 6\text{H}_2\text{O}$  or  $\text{PdCl}_2$  solution [11-12]. Electrochemical measurements were made with a standard three-electrode cell used for CV and CA. A platinum wire and Ag/AgCl (in 3 M KCl saturated) were used as auxiliary and reference electrodes, respectively. Electrochemical measurements were studied in a  $\text{N}_2$  saturated 0.5 M  $\text{H}_2\text{SO}_4$  solution with and without 0.5 M  $\text{CH}_3\text{OH}$  solution. The CVs test was recorded between -0.4 and 1.0 V at a scan rate of 50 mV/s, and the stability was recorded by CAs at a specific potential of these catalysts (maximum forward potentials scans ( $E_p$ ) for 3600 s.

### Characterization

The thickness of the GO support was measured by AFM (Veeco). Morphologies of the prepared catalyst were monitored by FE-SEM (JEOL JSM-6335F) and TEM (JEOL JEM-2010) with EDS. Structural characterization of the catalysts were investigated by FT-IR spectroscopy (TENSOR-27, Bruker).

## RESULTS AND DISCUSSION

### Catalyst Characterization

The topographic image of the GO support obtained by the AFM technique is shown in Fig. 1(a). The 3D image of the GO surface can be seen in Fig. 1 (b). The height profile presented in Fig. 1 (c) shows a thickness of ca. 2.673 nm indicating a single layer of exfoliated GO [13-14]. The surface roughness may be an impurity from the GO surface [8].

The morphologies of the catalysts were further studied with FE-SEM and TEM techniques. Fig. 2 (a)-(d) shows the surface topmost layers of the  $\text{TiO}_2$ , GO, 2Pt-GO and 2Pt/ $\text{TiO}_2$ -GO catalysts. The  $\text{TiO}_2$  with spherical shapes and various particle sizes is shown in Fig. 2 (a) [15-16]. The GO (Fig. 2 (b)) shows single layer sheets with rather smooth surface, while the 2Pt-GO and 2Pt/ $\text{TiO}_2$ -GO composites show rough surfaces. It can also be seen from Fig. 2 (c) and (d) that

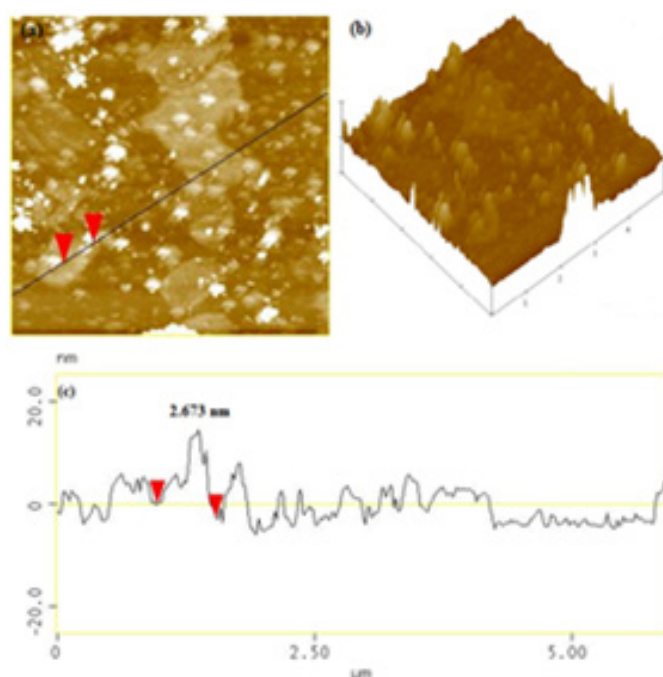


**Figure 1** AFM image of GO (a) 2D, (b) 3D and (c) the corresponding height profile.

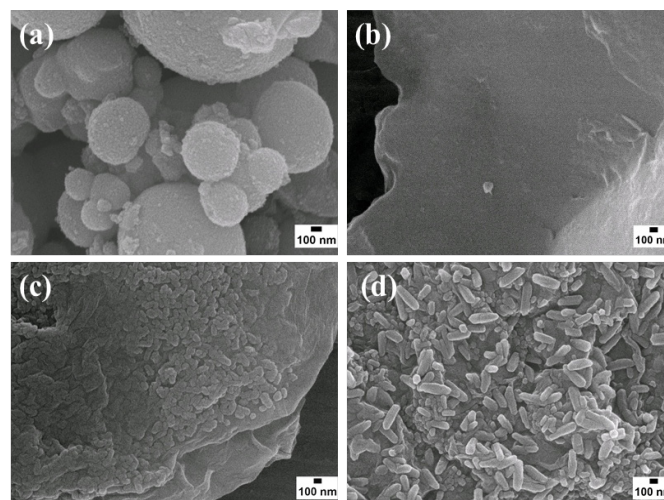


**Figure 2** FE-SEM images of  $\text{TiO}_2$  particles (a), GO (b), 2Pt-GO (c) and 2Pt/ $\text{TiO}_2$ -GO (d).

Pt nanoparticles are dispersed on the GO and  $\text{TiO}_2$ -GO supports respectively.

TEM images of GO,  $\text{TiO}_2$ -GO, 2Pt-GO and 2Pt/ $\text{TiO}_2$ -GO catalysts are shown in Fig. 3 (a)-(d), respectively. The GO support presents as a single layer sheet with smooth surface, consistent with the SEM result. After adding  $\text{TiO}_2$ , the  $\text{TiO}_2$  particles were attached to the GO support. The EDS spectrum of the 2Pt/ $\text{TiO}_2$ -GO (Fig. 3 (e)) confirms the existence of Pt and Ti elements. The presence of Cu element arises from the copper grid for TEM study. The particle size distribution of Pt on the GO and  $\text{TiO}_2$ -GO supports are shown in Fig. 4. The mean particle sizes of Pt on the GO and  $\text{TiO}_2$ -GO supports are about 4.09 and 3.23 nm, respectively. The small particle size implies a higher catalytic activity. Therefore, enhanced electrocatalytic activity for methanol oxidation is expected from the 2Pt/ $\text{TiO}_2$ -GO catalyst due to small Pt particle size and lower agglomeration of Pt nanoparticles on the  $\text{TiO}_2$ -GO support [4, 17-18].

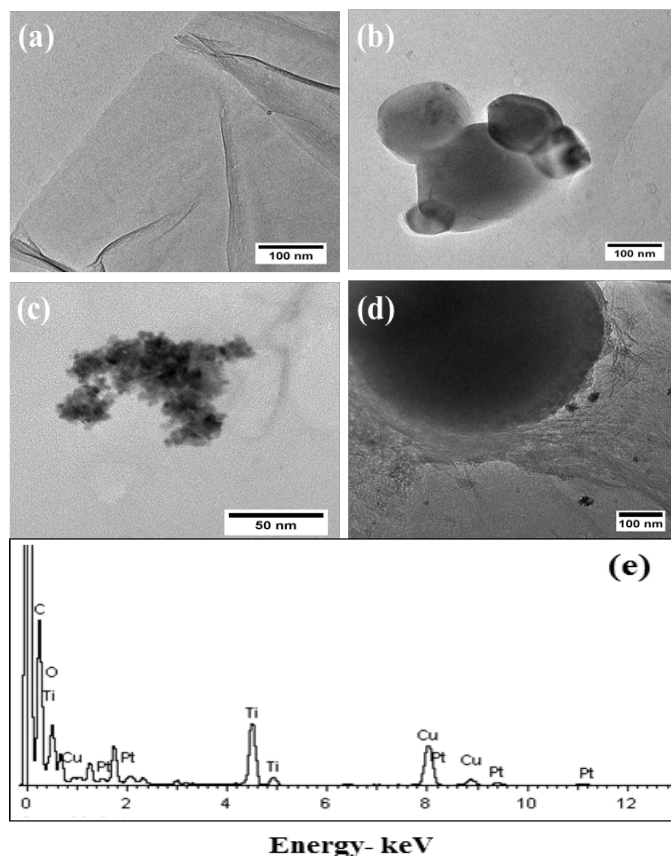


**Figure 3** TEM images of GO (a), TiO<sub>2</sub>-GO (b), 2Pt-GO (c), 2Pt/TiO<sub>2</sub>-GO (d) and EDS spectrum of 2Pt-TiO<sub>2</sub>-GO (e).

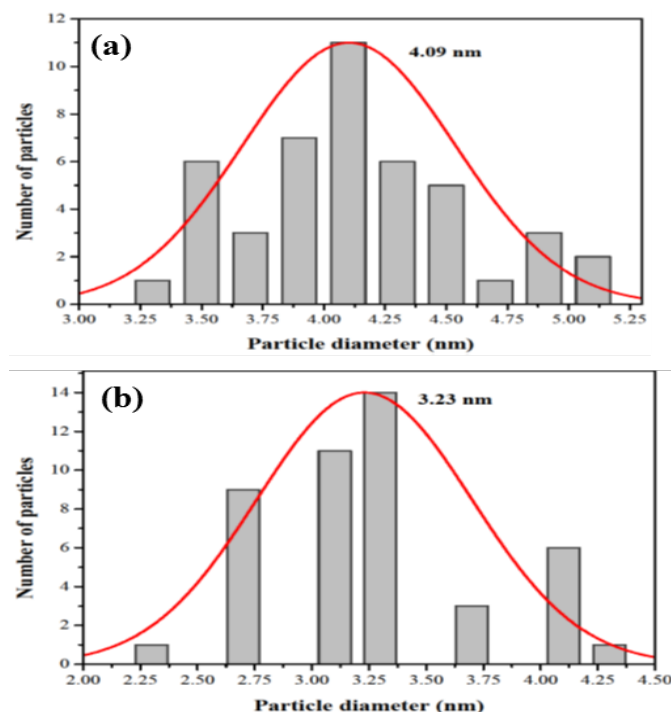


**Figure 4** Histogram of particle size distribution for 2Pt-GO (a) and 2Pt/TiO<sub>2</sub>-GO (b).

The FT-IR spectra of GO, TiO<sub>2</sub>-GO and TiO<sub>2</sub> are shown in Figure 5. The GO displays the characteristic absorption band *ca.* 1385 cm<sup>-1</sup> corresponding to the C-O carboxy group. The peaks at 1724 cm<sup>-1</sup> and

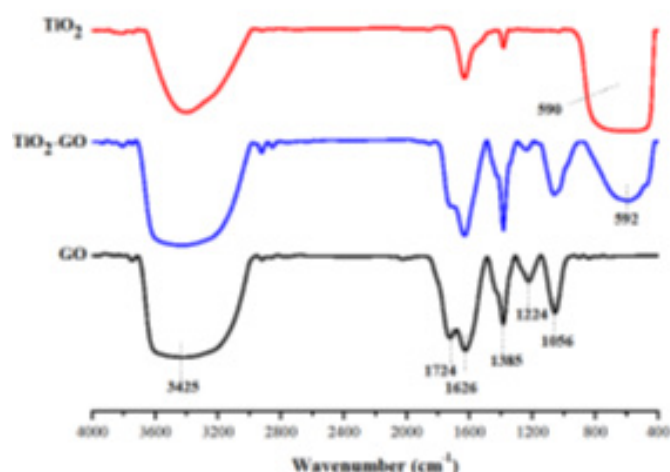


**Figure 5** The FT-IR spectra of GO, TiO<sub>2</sub>-GO and TiO<sub>2</sub> composites.

1056 cm<sup>-1</sup> correspond to the C=O and C-OH stretching vibrations of the COOH group, respectively. The band at 3400 cm<sup>-1</sup> and 1626 cm<sup>-1</sup> are associated with -OH stretching vibration and bending vibration modes of adsorbed water molecules indicating sp<sup>2</sup> characteristics [19-20]. Meanwhile, for the epoxy groups, a band *ca.* 1226 cm<sup>-1</sup> is observed. An additional peak due to Ti-O at *ca.* 590 cm<sup>-1</sup> can be found after adding TiO<sub>2</sub>, indicating a successful incorporation of TiO<sub>2</sub> on the GO surface.

#### Electrochemical characterization

The electrocatalytic properties of the prepared catalysts were evaluated by CVs in 0.5 M H<sub>2</sub>SO<sub>4</sub> (Fig. 6). The results demonstrate hydrogen adsorption/desorption (H<sub>ads/des</sub>) peaks in the potential ranging from -0.2 to -0.1 V. Double layer regions emerge between -0.1 and 0.5 V. Fig. 6 (a) and (b) show that the GO, TiO<sub>2</sub>-GO and 8Pd/TiO<sub>2</sub>-GO electrodes have no significant signal. However, the 2Pt/TiO<sub>2</sub>-GO and xPt2Pd/TiO<sub>2</sub>-GO provide remarkably higher hydrogen desorption (H<sub>des</sub>) intensity than that of 2Pt-GO. Interestingly, two distinct peaks from H<sub>des</sub> and another H<sub>ads</sub> peak at -0.2 V are found from xPt2Pd/TiO<sub>2</sub> on GO. The integrated area of the H<sub>des</sub> peaks represents an electrochemical surface area (ECSA) of the catalysts according to the following standard equation [22]:

$$\text{ECSA} = Q_{\text{H}} (\mu\text{C}\cdot\text{cm}^{-2}) / [210 \mu\text{C}\cdot\text{cm}^{-2} \times \text{Pt loading} (\text{mg}\cdot\text{cm}^{-2})] \quad (4)$$

where  $Q_{\text{H}}$  is the average of hydrogen adsorbed on (or desorbed from) the Pt surface determined by integrating the curves from -0.4 to 1.0 V, the value of 210  $\mu\text{C}\cdot\text{cm}^{-2}$  is the charge of a single hydrogen atom adsorbed on a single Pt atom assuming a monolayer coverage of atomic H on the Pt surface and Pt loading is the mass of Pt deposited on the working electrode ( $\text{mg}\cdot\text{cm}^{-2}$ ). ECSA values in Table 1 indicate that the ECSA increases with respect to the amount of Pt. Interestingly, adding 2 cycles of Pd to the Pt catalyst could further increase the ECSA of the prepared catalysts.

Methanol oxidation activities of the prepared catalysts are illustrated in Fig. 7. The 2Pt/TiO<sub>2</sub>-GO electrode shows notable catalytic activity, displaying outstanding current peaks for oxidation in both the positive and negative potential scans. In Fig. 7 (a), the  $I_{\text{f}}$  and  $I_{\text{b}}$  values of 2Pt/TiO<sub>2</sub>-GO are 1.36 and 0.98 mA·cm<sup>-2</sup> which are higher than those of 2Pt-GO (0.57 and 0.35 mA·cm<sup>-2</sup>). Although the  $I_{\text{f}}/I_{\text{b}}$  ratio of 2Pt/TiO<sub>2</sub>-GO (1.38) is slightly lower than that of 2Pt-GO (1.63), the  $I_{\text{f}}$  of 2Pt/TiO<sub>2</sub>-GO is incredibly high. For the Pt and Pd bi-metallic catalysts (xPt2Pd/TiO<sub>2</sub>-GO), the methanol oxidation activity of the samples increases as Pt content increases. In addition,

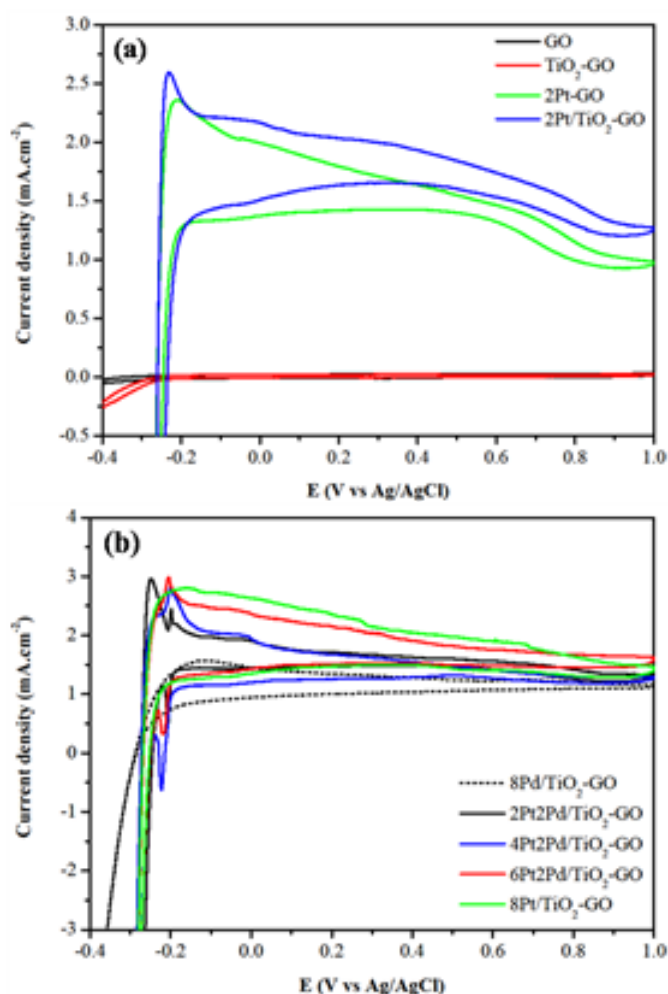


**Figure 6** CVs of GO, TiO<sub>2</sub>-GO, 2Pt-GO and 2Pt/TiO<sub>2</sub>-GO (a), xPt<sub>2</sub>Pd/TiO<sub>2</sub>-GO; x = 2, 4, 6 and 8 (b) in 0.5 M H<sub>2</sub>SO<sub>4</sub> solution at scan rate 50 mV/s.

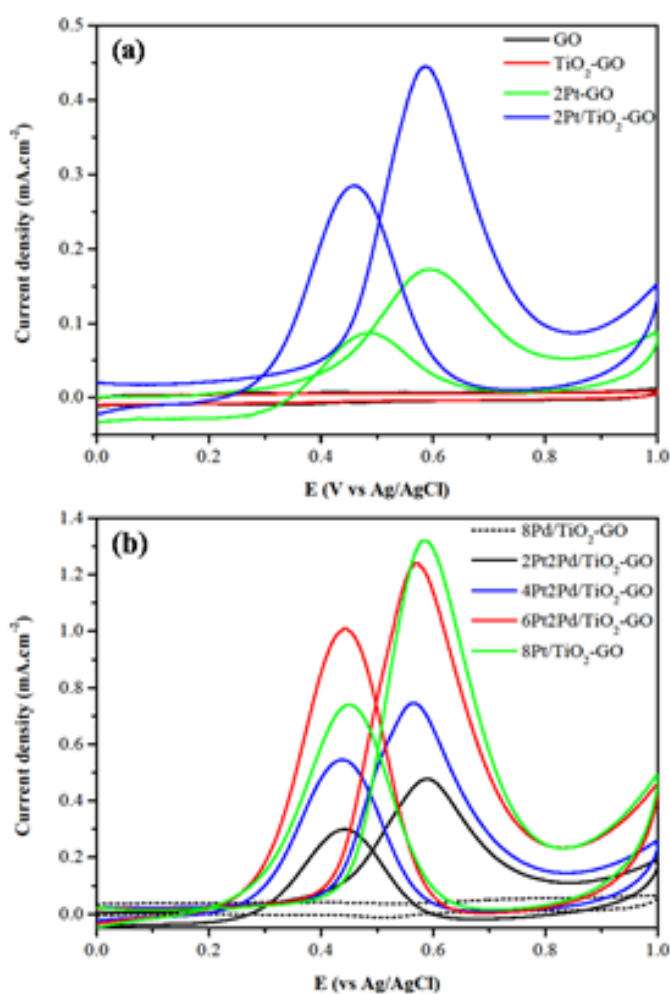


**Figure 7** CVs of GO, TiO<sub>2</sub>-GO, 2Pt-GO and 2Pt/TiO<sub>2</sub>-GO (a), xPt<sub>2</sub>Pd/TiO<sub>2</sub>-GO; x = 2, 4, 6 and 8 (b) in 0.5 M CH<sub>3</sub>OH and a 0.5 M H<sub>2</sub>SO<sub>4</sub> solution at scan rate 50 mV/s.

**Table 1** Electrochemical analysis of catalysts in methanol oxidation.

Catalyst	ECSA (cm <sup>2</sup> /mg)	E <sub>onset</sub> (V)	I <sub>r</sub> (mA/cm <sup>2</sup> )	E <sub>f</sub> (V)	I <sub>b</sub> (mA/cm <sup>2</sup> )	E <sub>b</sub> (V)	I <sub>r</sub> /I <sub>b</sub> ratio
2Pt-GO	33.71	0.45	0.57	0.59	0.35	0.47	1.63
2Pt/TiO <sub>2</sub> -GO	37.10	0.44	1.36	0.59	0.98	0.46	1.38
8Pd/TiO <sub>2</sub> -GO	-	-	-	-	-	-	-
2Pt <sub>2</sub> Pd/TiO <sub>2</sub> -GO	43.66	0.41	1.47	0.59	1.11	0.44	1.32
4Pt <sub>2</sub> Pd/TiO <sub>2</sub> -GO	72.71	0.41	2.36	0.57	1.83	0.44	1.29
6Pt <sub>2</sub> Pd/TiO <sub>2</sub> -GO	104.58	0.41	4.00	0.57	3.63	0.44	1.10
8Pt/TiO <sub>2</sub> -GO	127.80	0.41	4.07	0.58	2.65	0.45	1.53

the oxidation activity of bi-metallic 6Pt<sub>2</sub>Pd/TiO<sub>2</sub>-GO is comparable to mono-metallic 8Pt/TiO<sub>2</sub>-GO (Fig. 7 (b)). Although 8Pt/TiO<sub>2</sub>-GO provides higher ECSA than 6Pt<sub>2</sub>Pd/TiO<sub>2</sub>-GO, the I<sub>r</sub> is not significantly different from that of 6Pt<sub>2</sub>Pd/TiO<sub>2</sub>-GO. The results imply that the preparation of bi-metallic catalyst used in this study helps reduce Pt

loading content in the electrocatalyst.

It has been reported [8, 21] that the reaction mechanism of methanol oxidation on a Pt electrode in acidic solution includes parallel and consecutive oxidations as follows:

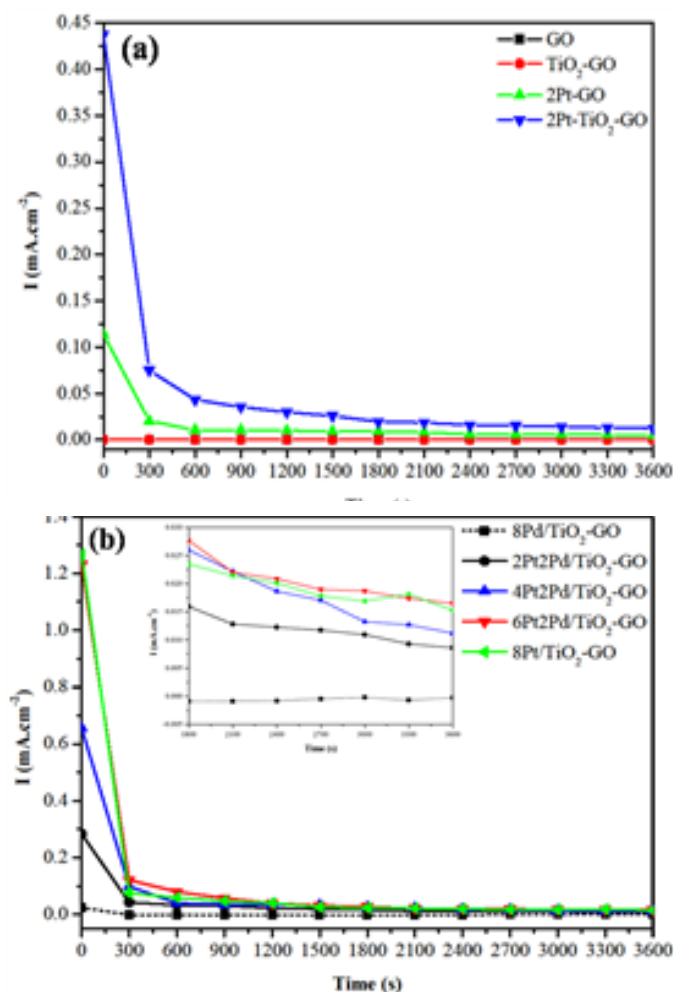
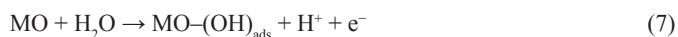


**Figure 8** Chronoamperometric curves of GO, TiO<sub>2</sub>-GO, 2Pt-GO and 2Pt/TiO<sub>2</sub>-GO (a), xPt2Pd/TiO<sub>2</sub>-GO; x = 2, 4, 6 and 8 (b) in 0.5 M CH<sub>3</sub>OH and a 0.5 M H<sub>2</sub>SO<sub>4</sub> solution at specific potentials of these catalysts, 3600 s.



Further oxidation of CO to CO<sub>2</sub> is generally difficult on Pt catalyst due to the deficiency of active oxygen on the surface. CO acts as poisoning species to Pt. It strongly adsorbs on the Pt surfaces and blocks the surfaces from further oxidation of CO to CO<sub>2</sub>, thus reducing the electrocatalytic activity of the catalyst. When Pt is incorporated with metal oxide, the enhancement of CO oxidation can easily be obtained by reaction with OH species on the metal oxide surfaces as in equations (7) and (8):



The OH<sub>ads</sub> species on metal oxide can transform CO-like poisoning species (CO<sub>ads</sub>) on Pt to CO<sub>2</sub>, thus releasing the active sites on Pt for further electrochemical reaction. It is rational to expect that the incorporation of the oxygen storage material into the TiO<sub>2</sub>-GO support could introduce the local oxygen concentration, thereby increasing the methanol electro-oxidation activity. An addition of Pd on xPt/TiO<sub>2</sub>-GO electrodes can obviously lower an onset potential

because water dehydrogenation on Pd to form Pd-OH<sub>ads</sub> is beneficial for enhanced CO oxidation, thus easily regaining the active metal surface. Without Pd, the water hydrogenation on Pt occurs at a higher potential, making the overall oxidation process on pure Pt sluggish [23-24].

Chronoamperometric curves (CAs) of 2Pt-GO and 2Pt/TiO<sub>2</sub>-GO electrocatalysts in 0.5 M CH<sub>3</sub>OH in 0.5 M H<sub>2</sub>SO<sub>4</sub> solution are displayed in Fig. 8 at a specific potential of these catalysts (vs Ag/AgCl) for 3600 s. Methanol was constantly oxidized at the electrocatalyst surface and the reaction intermediates such as CO<sub>ads</sub> were obtained. These species will accumulate on the catalytic surfaces if the kinetics of removal reactions cannot be accomplished fast enough for the methanol oxidation. This helps explain the sharp decrease in oxidation current density at the first few seconds, followed by a steady state current in Fig. 8 (a) and (b). From Fig. 8 (a), the oxidation current density of 2Pt/TiO<sub>2</sub>-GO (0.019 mA/cm<sup>2</sup>) is still higher than that of 2Pt-GO catalyst after 2100 s, indicating long-term stability of 2Pt/TiO<sub>2</sub>-GO [5, 25]. In Fig. 8 (b), the current densities of all catalysts quickly decayed and after long term reaction the current intensities were steady in the following order: 6Pt2Pd/TiO<sub>2</sub>-GO > 8Pt/TiO<sub>2</sub>-GO > 4Pt2Pd/TiO<sub>2</sub>-GO > 2Pt2Pd/TiO<sub>2</sub>-GO. It is clear that the combination of metal oxide and Pd creates a synergistic effect on the catalyst system by lowering the oxidation potential and increasing the electrocatalytic stability for methanol oxidation reaction.

## CONCLUSION

2Pt/TiO<sub>2</sub>-GO was successfully prepared and its application for methanol oxidation was also investigated in the present work. IR spectra confirmed that the metal oxides were loaded on the GO surface while AFM showed the thin film of the prepared GO. FE-SEM and TEM indicated that the catalyst preparation method used in this study could provide small Pt nanoparticles with narrow size distribution. EDS also confirmed the presence of Pt and Ti elements in the composite catalyst. Among the prepared catalysts, 8Pt/TiO<sub>2</sub>-GO showed higher current density as well as lower onset potential and higher stability than those observed from 2Pt-GO. Moreover, the electrocatalytic activities of bi-metallic xPt2Pd/TiO<sub>2</sub>-GO electrodes were found to depend on the Pt content. The addition of Pd reduced the onset potential and increased catalyst stability. Thus, the surface modification of GO with Pt, Pd and TiO<sub>2</sub> could produce a promising anode catalyst for direct methanol fuel. However, the actual content of those elements has to be studied further.

## ACKNOWLEDGEMENTS

The authors thank the Center of Excellence for Innovation in Chemistry (PERCH-CIC), Commission on Higher Education, Ministry of Education, Graduate School of Chiang Mai University, Electrochemical for Alternative Energy Research Laboratory (EAER LAB), the Centre of Excellence in Materials Science and Technology, Faculty of Science, Chiang Mai University (CoE) for financial support.

## REFERENCES

1. Z. Yang, J. Ren, Z. Zhang, X. Chen, G. Guan, L. Qiu, Y. Zhang and H. Peng, Recent advancement of nanostructured carbon for energy applications, *Chem. Rev.*, **2015**, 115, 5159-5223.
2. L. Carrette, K. A. Friedrich and U. Stimming, Fuel cells—fundamentals and applications, *Fuel cells.*, **2001**, Vol.1, 5-39.
3. S. K. Kamarudin, F. Achmad and W. R. W. Daud, Overview on the application of direct methanol fuel cell (DMFC) for portable

- electronic devices, *Int. J. Hydrogen Energy*, **2009**, 34, 6902-6916.
- N. Kakati, J. Maiti, S. H. Lee, S. H. Jee, B. Viswanathan and Y. S. Yoon, Anode catalysts for direct methanol fuel cells in acidic media: do we have any alternative for Pt or Pt-Ru?, *Chem. Rev.*, **2014**, 114, 12397-12429.
  - R. M. A. Hameed, R. S. Amin, K. M. El-Khatib and A. E. Fetohi, Preparation and characterization of Pt-CeO<sub>2</sub>/C and Pt-TiO<sub>2</sub>/C electrocatalysts with improved electrocatalytic activity for methanol oxidation, *Appl. Surf. Sci.*, **2016**, 367, 382-390.
  - M. Khan, A.B. Yousaf, M. Chen, C. Wei, X. Wu, N. Huang, Z. Qi, L. Li, Mixed-phase Pd-Pt bimetallic alloy on graphene oxide with high activity for electrocatalytic applications, *J. Power Sources*, **2015**, 282, 520-528.
  - W. S. Hummers Jr and R. E. Offeman, Preparation of graphitic oxide, *J. Am. Chem. Soc.*, **1958**, 80, 1339-1339.
  - Q. Sun, S.-J. Park and S. Kim, Preparation and electrocatalytic oxidation performance of Pt/MnO<sub>2</sub>-graphene oxide nanocomposites, *Ind. Eng. Chem. Res.*, **2015**, 26, 265-269.
  - Y. Zhu, S. Murali, W. Cai, X. Li, J. W. Suk, J. R. Potts and R. S. Ruoff, Graphene and graphene oxide: synthesis, properties, and applications, *Adv. Mater.*, **2010**, 22, 3906-3924.
  - S. Themsirimongko, N. Promsawan and S. Saipanya, Noble Metal and Mn<sub>3</sub>O<sub>4</sub> Supported Carbon Nanotubes: Enhanced Catalysts for Ethanol Electrooxidation, *Int. J. Electrochem. Sci.*, **2016**, 11, 967-982.
  - A. Pinitchaisakula, S. Themsirimongkon, N. Promsawan, P. Weankeaw, K. Ounnunkad and S. Saipanya, An Investigation of a Polydopamine-Graphene Oxide Composite as a Support for an Anode Fuel Cell, *Electro catalysis*, **2016**, 1-10.
  - Y. Zhao, L. Fan, H. Zhong, Y. Li and S. Yang, Platinum nanoparticle clusters immobilized on multiwalled carbon nanotubes: Electrodeposition and enhanced electrocatalytic activity for methanol oxidation, *Adv. Funct. Mater.*, **2007**, 17, 1537-1541.
  - J. Chen, H. Peng, X. Wang, F. Shao, Z. Yuan and H. Han, Graphene oxide exhibits broad-spectrum antimicrobial activity against bacterial phytopathogens and fungal conidia by intertwining and membrane perturbation, *Nanoscale*, **2014**, 6, 1879-1889.
  - T. Lammel, P. Boisseaux, M.-L. Fernández-Cruz and J. M. Navas, Internalization and cytotoxicity of graphene oxide and carboxyl graphene nanoplatelets in the human hepatocellular carcinoma cell line Hep G2, *Part. Fibre Toxicol.*, **2013**, 10, 27.
  - M. Andersson, L. Österlund, S. Ljungström and A. Palmqvist, Preparation of nanosize anatase and rutile TiO<sub>2</sub> by hydrothermal treatment of microemulsions and their activity for photocatalytic wet oxidation of phenol, *J. Phys. Chem. B*, **2002**, 106, 10674-10679.
  - R. Vijayalakshmi and V. Rajendran, Synthesis and characterization of nano-TiO<sub>2</sub> via different methods, *Arch. App. Sci. Res.*, **2012**, 4, 1183-1190.
  - H. Song, X. Qiu and F. Li, Effect of heat treatment on the performance of TiO<sub>2</sub>-Pt/CNT catalysts for methanol electro-oxidation, *Electrochim. Acta.*, **2008**, 53, 3708-3713.
  - Y. Qu, Y. Gao, F. Kong, S. Zhang, L. Du and G. Yin, Pt-rGO-TiO<sub>2</sub> nanocomposite by UV-photoreduction method as promising electrocatalyst for methanol oxidation, *Int. J. Hydrogen Energy*, **2013**, 38, 12310-12317.
  - C. Patomnetikul, S. Thongtem and S. Narksitipan, Characterization of GO and TiO<sub>2</sub>-GO composites prepared by using microwave technique, *Int. Soc. Opt. Photo.*, **2014**, 923406-923406.
  - M. R. Gaeni, M. Tohidian, M. Sasani Ghamsari and M. H. Majles Ara, Synthesis of graphene oxide-TiO<sub>2</sub> nanocomposite as an adsorbent for the enrichment and determination of rutin, *J. Nanomed.*, **2015**, 2, 269-272.
  - Y. Yuying, Z. Zhang and H. Zhongai, Activity improvement of Pt/C catalysts by adding CeO<sub>2</sub> nanoparticles, *J. Rare Earths*, **2011**, 29, 58-63.
  - Y. Li, W. Gao, L. Ci, C. Wang, P.M. Ajayan, Catalytic performance of Pt nanoparticles on reduced graphene oxide for methanol electro-oxidation, *Carbon*, **2010**, 48, 1124-1130.
  - Z.-x. Cai, C.-c. Liu, G.-h. Wu, X.-m. Chen, X. Chen, Green synthesis of Pt-on-Pd bimetallic nanodendrites on graphene via in situ reduction, and their enhanced electrocatalytic activity for methanol oxidation, *Electrochimica Acta.*, **2014**, 127, 377-383.
  - Y. Liu, M. Chi, V. Mazumder, K.L. More, S. Soled, J.D. Henao, S. Sun, Composition-controlled synthesis of bimetallic PdPt nanoparticles and their electro-oxidation of methanol, *Chemistry of Materials*, **2011**, 23, 4199-4203.
  - R. M. Hameed, R. S. Amin, K. M. El Khatib and A. E. Fetohi, Influence of Metal Oxides on Platinum Activity towards Methanol Oxidation in H<sub>2</sub>SO<sub>4</sub> solution, *Chem. Phys. Chem.*, **2016**, 17, 1054-1061.